A novel multilaminated composite cathode for solid oxide fuel cells

L. dos Santos-Gómez[a], J.M. Porras-Vázquez[a], F. Martín[b], J.R. Ramos-Barrado[b], E.R. Losilla[a], D. Marrero-López[b,*]

[a]Universidad de Málaga, Departamento de Química Inorgánica, 29071-Málaga, Spain

[b]Universidad de Málaga, Departamento de Física Aplicada I, Laboratorio de Materiales y Superficies, 29071-Málaga, Spain

ABSTRACT

A novel electrode architecture consisting in alternating layers of $La_{0.6}Sr_{0.4}Co_{0.2}Fe_{0.8}O_{3-\delta}$ (LSCF) and $Ce_{0.9}Gd_{0.1}O_{1.95}$ (CGO) is prepared for the first time by spray-pyrolysis deposition and investigated as cathode material for Solid Oxide Fuel Cells (SOFCs). Cathodes with different number of LSCF/CGO bilayers (N=0, 3 and 5) are prepared and characterized. The multilaminated cathodes are highly porous with connected vertical channels and display an unusual undulated morphology, which increases the contact area between CGO and LSCF materials. The oxygen reduction reaction activity has been investigated by impedance spectroscopy, obtaining improved values of polarization resistance as the number of bilayers increases due to extended three-phase-boundary (TPB) length for the oxygen reduction reactions.

Keywords: spray-pyrolysis; solid oxide fuel cells; $Ce_{0.9}Gd_{0.1}O_{1.95}$; $La_{0.6}Sr_{0.4}Co_{0.2}Fe_{0.8}O_{3-\delta}$

* Corresponding author.

E-mail address: marrero@uma.es (David Marrero-López)

Present address: Dpto. de Física Aplicada I, Facultad de Ciencias, Campus de Teatinos, Universidad de Málaga, 29071-Málaga, Spain.

Tel: +34 952137057, Fax: +34 952132382

1. Introduction

The application of Solid Oxide Fuel Cells (SOFCs) at low operating temperatures is mainly hindered by the poor electrocatalytic activity of the cathode towards the oxygen reduction reactions (ORR) [1-5]. Different materials with single-perovskite, layered-perovskite and Ruddlesden-Popper type structures, such as $La_{0.6}Sr_{0.4}Co_{0.2}Fe_{0.8}O_{3-\delta}$ (LSCF), $PrBaCo_2O_{5+\delta}$ and $La_2NiO_{4+\delta}$, respectively, have been investigated as an alternative to the commonly used $La_{0.8}Sr_{0.2}MnO_{3-\delta}$ cathode, which exhibits low ionic conductivity to operate efficiently at reduced temperatures [6-9].

On the other hand, it is well known that the electrode performance depends not only on the intrinsic properties of the material, but also by the microstructure. However, it is difficult to achieve an optimized electrode microstructure with small particle size and high porosity due to the high co-sintering temperatures required by the conventional fabrication methods, such as screen-printing, dip-coating, spin-coating, etc., which lead to an excessive grain growth and consequently a loss of performance [10]. Novel fabrication methodologies and electrode architectures have been employed to improve the electrocatalytic activity of the cathodes, including, for example, surface modification by infiltration, sacrificial template and electrospinning [11-14]. Nevertheless, these methods are unsuitable for large scale production due to the multiple fabrication steps required. In contrast, spray-pyrolysis is a simple, economic and easily scalable technique for the preparation of nanostructured electrodes over large areas [15]. This technique has been employed to obtain cathodes with a variety of morphologies, i.e. dense, porous and with graded composition [16,17]. An alternative approach to improve the electrode performance is the addition of a second phase with high ionic conductivity, typically the same as the electrolyte, to extend the TPB length [1,3].

Herein, a novel electrode architecture, consisting in alternating layers of LSCF and CGO, is proposed for the first time. Electrodes with different number of bilayers are prepared by spray-pyrolysis deposition and the structure, microstructure and electrical properties are investigated.

2. Experimental

2.1. Materials preparation

$Ce_{0.9}Gd_{0.1}O_{1.95}$ (CGO, Rhodia) pellets of 10 and 1 mm of diameter and thickness, respectively, were used as electrolyte support, which were obtained by pressing the powders into disks and then sintering at 1400 ºC for 4 h. Two different precursor solutions of $La_{0.6}Sr_{0.4}Co_{0.2}Fe_{0.8}O_{3-\delta}$ and $Ce_{0.9}Gd_{0.1}O_{1.95}$ with concentration of 0.025 mol L^{-1} were prepared by dissolving the corresponding nitrate salts: $Ln(NO_3)_3 \cdot 6H_2O$ (Ln=La, Ce and Gd), $Sr(NO_3)_2$, $Co(NO_3)_2 \cdot 6H_2O$ and $Fe(NO_3)_3 \cdot 9H_2O$ (Sigma-Aldrich, purity >99%) in distilled water. Ethylenediaminetetraacetic acid was added as chelating agent with a molar EDTA:metal ratio of 0.25 to prevent phase segregation and heterogeneity.

The precursor solutions, supplied by two independent syringe pumps, were alternately atomized in a spray-nozzle using air as carrier gas with a solution flow rate of 0.02 L h^{-1}. The deposition was made through a circular shadow mask of 0.2 cm^2 at a temperature of 350 ºC. Electrodes with different number of LSCF/CGO bilayers (N=0, 3 and 5) were obtained, where N=0 represents the LSCF blank cathode, whereas the cathode architecture for N=3 is comprised of three bilayers: LSCF/CGO/LSCF/CGO/LSCF/CGO and similarly for N=5. In order to compare the different electrode architectures, the deposition time of the CGO layer was fixed at 5 min, while the deposition time of the LSCF layer was 7, 15 and 60 min for N=5, 3 and 0, respectively. In this way, the total deposition time was 60 min for all samples. Finally, the samples were thermally treated in a furnace in air at 800 ºC for 2 h to obtain the crystalline phases.

The structure and composition of the electrodes was studied by X-ray powder diffraction (XRD) with a PANalytical Empyrean diffractometer. The microstructure was observed by electron microscopy, SEM (FEI, Helios Nanolab 650), equipped with a Tomahawk focused ion beam, a platinum gas injection system and an energy dispersive X-ray spectrometer (EDX, X-Max Oxford). The 3D reconstruction was performed with Avizo Software (FEI Visualization Sciences Group).

The electrode polarization resistance was determined by impedance spectroscopy (Solartron 1260-FRA) between 300 and 650 ºC in atmospheric air as described elsewhere [18]. The spectra were analyzed by equivalent circuits using the ZView software (Scribner).

3. Results and discussion

XRD patterns show that the crystalline compounds are obtained at 800 ºC without any detectable impurity (Fig. 1a). Three different phases are observed in the patterns, which are ascribed to the CGO substrate, with narrow diffraction peaks, and the LSCF/CGO bilayers, where both phases present broad peaks due to their nanocrystalline nature. The data are analyzed by the Rietveld method in the cubic space groups $Fm\bar{3}m$ and $Pm\bar{3}m$ for CGO and LSCF, respectively. It should be commented that bulk LSCF crystallizes with rhombohedral symmetry (s.g. $R\bar{3}c$); however, the cubic structure is stabilized for nanocrystalline samples [19]. An example of the Rietveld plot is given in Fig. 1b and the structural results are compared in Table 1. As can be observed, the unit cell volume is similar for the different phases and electrode architectures, indicating that the same materials are obtained, regardless of the number of layers N. The average crystallite size of LSCF, estimated by using the Scherrer´s equation, decreases with increasing N from 34 to 23 nm (Table 1). This phenomenon is mainly attributed to the presence of CGO as secondary phase, which limits the cation diffusion, and consequently, the grain growth rate decreases.

Table 1. Structural parameters of the electrodes and average crystallite size of LSCF.

	Unit cell volume/Z (Å)			**d_{LSCF} (nm)**	**R_{wp}(%)**
N	**CGO substrate**	**CGO electrode**	**LSCF electrode**		
0	39.80(1)	-	58.63(1)	34	3.70
3	39.80(1)	39.81(3)	58.51(1)	29	3.51
5	39.79(1)	39.80(2)	58.70(1)	23	3.67

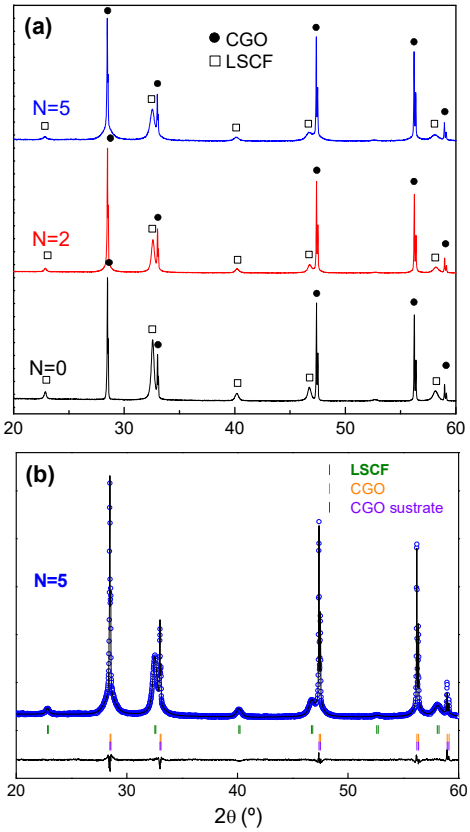

Fig. 1. (a) XRD patterns of LSCF/CGO cathodes deposited on CGO electrolyte with different number of bilayers N. (b) Rietveld plot for N=5.

The microstructure of the cathodes with N=0 and N=5 are shown in Fig. 2. The blank LSCF cathode consists in a multilaminated microstructure, typical of a spinodal phase decomposition after removing the organic residues by heat treatment [20]. This morphology is different to that previously observed in LSCF cathodes prepared from nitrate precursors, suggesting that the spinodal microstructure is associated with the addition of EDTA [19]. It is also interesting to highlight that the grain size is larger on the surface than in the inner electrode, leading to a gradual decrease of the grain size over the layer thickness, which is attributed to a temperature gradient during the thermal treatment.

The sample with N=5 shows an undulated and multilaminated morphology, where the elements of both compounds are well differentiated by EDX analysis (Fig. 2b). It has to be noticed that the cathode is coated with Pt to protect the sample before FIB preparation. This unusual undulated microstructure is caused by the different shrinkage and bending of the layers during the sintering process, increasing dramatically the contact area between the LSCF and CGO phases. The 3D reconstruction (Fig. 2c) reveals that the laminated electrodes are porous (~35% porosity) and the presence of vertical macropore channels guarantees an

adequate oxygen diffusion inside the electrode (Fig. 2d). It is also worth noting that the CGO layers are not a barrier for the electronic conduction since the LSCF layers are connected through the macropore channels (Fig. 2b, see also the electronic annex in the online version of this article).

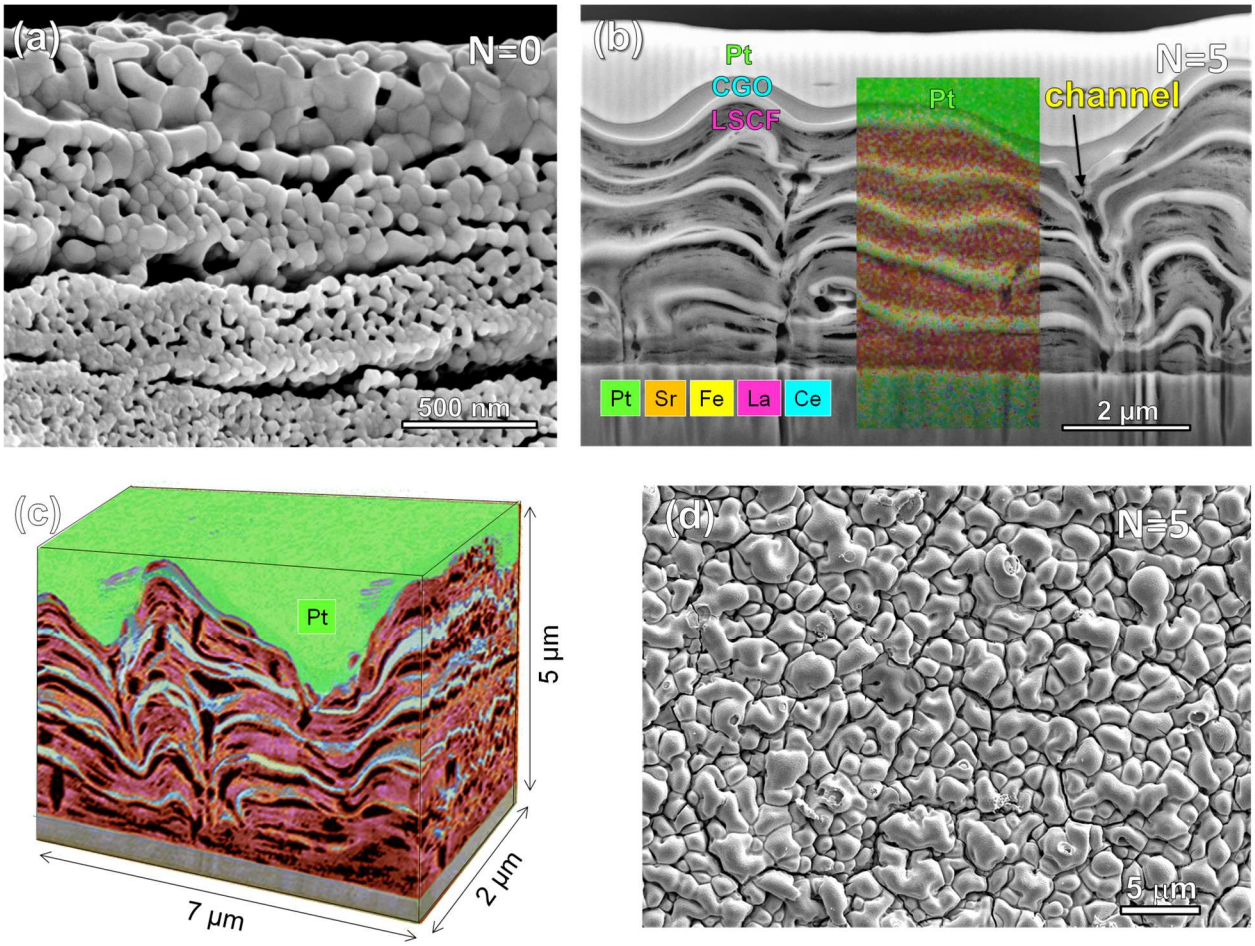

Fig. 2. (a) Cross-sectional SEM imagen of (a) blank cathode and (b) multilaminated cathode with N=5. (c) 3D reconstruction and (b) surface morphology of N=5.

The Nyquist plots for the different cathode architectures at 600 ºC are displayed in Fig. 3a. The most significant difference between them is a decrease of the overall polarization resistance with increasing N. All the plots show similar features and they are analyzed by considering an equivalent circuit formed by two serial (RQ) elements, being R a resistance in parallel with a constant-phase-element Q. The relaxation frequency and capacitance values of the high and the low frequency contributions are similar for the different electrodes, indicating that the same processes are involved in the cathodes, regardless of the number of alternating layers N. The capacitance values, i.e. 0.5 and 5 mF cm^{-2} for the high and low frequency processes, respectively, are typical of charge transfer and oxygen dissociation adsorption, in accordance with

previous studies [21]. In addition, the low frequency contribution exhibits higher resistance than the low frequency one, indicating that the oxygen dissociation adsorption is the rate limiting step for the oxygen reduction reaction.

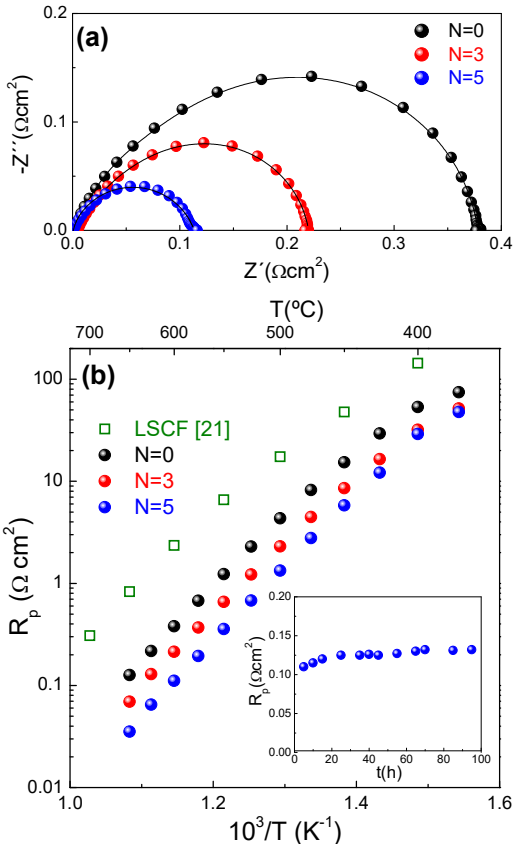

Fig. 3. (a) Nyquist plots of the different cathodes at 600 ºC in air. (b) Temperature dependence of the electrode polarization resistance. The inset of (b) shows the polarization resistance over time at 600 ºC.

The overall polarization resistance decreases as N increases from 0.38 Ω cm^2 for N=0 to 0.11 Ω cm^2 for N=5 at 600 ºC (Fig. 3b). These values of polarization resistance are relatively low compared to those obtained for LSCF screen-printing powders and infiltrated electrodes, 2.1 and 0.24 Ω cm^2 at 600 ºC, respectively [21,22]. Moreover, the polarization resistance is stable over time at 600 ºC, confirming the potential application of these electrodes at low operating temperatures (inset Fig. 2b). The improvement of the polarization resistance with increasing N is attributed to a larger TPB length due to a larger contact area between the LSCF and CGO layers. In addition, the LSCF particles in contact with CGO are less susceptible to surface carbonation, caused by superficial strontium segregation, which blocks the active sites for the oxygen reduction reaction [21,23]. Thus, the values of polarization resistance and stability could be further improved by increasing N.

Additional improvements could be made by varying the deposition temperature and the EDTA content. For instance, an increase of the deposition temperature would decrease the organic matter after the spray-pyrolysis deposition, minimizing the shrinkage and bending effects during the thermal treatment, and consequently, thinner layers with lower undulation could be obtained. The thickness of both CGO and LSCF layers can be tailored by varying the deposition time. For instance, shorter deposition times would result in thinner CGO layers, improving the electrical properties of the composite cathode. The influence of the EDTA content on the formation of the spinodal microstructure should also be investigated, which is interesting, since this increase the electrode porosity. Hence, this new electrode preparation strategy could be used to achieve different cathode and anode materials for SOFCs and other electrochemical devices with improved performance and stability.

4. Conclusions

A spray-pyrolysis deposition method has been employed to obtain a novel electrode architecture composed of alternating layers of LSCF and CGO. Multilaminated cathodes with high porosity and undulated morphology are obtained, maximizing the contact area between both materials, and consequently, the TPB sites for the oxygen reduction reactions. The polarization resistance decreases by increasing the number of bilayers from 0.38 to 0.11 Ω cm^2 for N=0 and 5, respectively, at 600 ºC.

Acknowledgements

This work has been supported by MINECO and FEDER though the RTI2018-093735-B-I00 and MAT2016-77648-R research grants (Spain). L. dos Santos-Gómez and J.M. Porras-Vázquez thank to the University of Malaga for the funding.

References

[1] Z. Gao, L.V. Mogni, E.C. Miller, J.G. Railsback, S.A. Barnett, A perspective on low-temperature solid oxide fuel cells, Energy Environ. Sci. 9 (2016) 1602-1644.

[2] Y. Zhang, R. Knibbe, J. Sunarso, Y. Zhong, W. Zhou, Z. Shao, Z. Zhu, Recent progress on advanced materials for solid-oxide fuel cells operating below 500 °C, Adv. Mater. 29 (2017) 1700132.

[3] A. Jun, J. Kim, J. Shin, G. Kim, Perovskite as a Cathode Material: A Review of its Role in Solid-Oxide Fuel Cell Technology, ChemElectroChem. 3 (2016) 511-530.

[4] B. Singh, S. Ghosh, S. Aich, B. Roy, Low temperature solid oxide electrolytes (LT-SOE): A review, J. Power Sources 339 (2017) 103-135.

[5] F.S. da Silva, T.M. de Souza, Novel materials for solid oxide fuel cell technologies: A literature review, Int. J. Hydrog. Energy 42 (2017) 26020-26036.

[6] M. Shao, Q. Chang, J.P. Dodelet, R. Chenitz, Recent Advances in Electrocatalysts for Oxygen Reduction Reaction, Chem. Rev. 116 (2016) 3594-3657.

[7] Y. Chen, W. Zhou, D. Ding, M. Liu, F. Ciucci, M. Tade, Z. Shao, Advances in Cathode Materials for Solid Oxide Fuel Cells: Complex Oxides without Alkaline Earth Metal Elements, Adv. Energy Mater. 5 (2015) 1500537.

[8] N. Mahato, A. Banerjee, A. Gupta, S. Omar, K. Balani, Progress in material selection for solid oxide fuel cell technology: A review, Prog. Mater. Sci. 72 (2015) 141-337.

[9] A. Jun, J. Kim, J. Shin, G. Kim, Perovskite as a Cathode Material: A Review of its Role in Solid-Oxide Fuel Cell Technology, ChemElectroChem 3 (2016) 511-530.

[10] M.R. Somalu, A. Muchtar, W.R.W. Daud, N.P. Brandon, Screen-printing inks for the fabrication of solid oxide fuel cell films: A review, Renew. Sust. Energ. Rev. 75 (2017) 426-439.

[11] D. Ding, X. Li, S. Lai, K. Gerdes, M. Liu, Enhancing SOFC, Cathode Performance by Surface Modification Through Infiltration, Energy Environ. Sci. 7 (2014) 552-575.

[12] N. Hedayat, Y. Du, H. Ilkhani, Review on fabrication techniques for porous electrodes of solid oxide fuel cells by sacrificial template methods, Renew. Sust. Energ. Rev. 77 (2017) 1221-1239.

[13] A.M. Abdalla, S. Hossain, A.T. Azad, P.M.I. Petra, F. Begum, S.G. Eriksson, A.K. Azad, Nanomaterials for solid oxide fuel cells: A review, Renew. Sust. Energ. Rev. 82 (2018) 353-368.

[14] S.T. Aruna, L.S. Balaji, S.S. Kumar, B.S. Prakash, Electrospinning in solid oxide fuel cells – A review, Renew. Sust. Energ. Rev. 67 (2017) 673-682.

[15] C. Guild, S. Biswas, Y. Meng, T. Jafari, A.M. Gaffney, S.L. Suib, Perspectives of spray pyrolysis for facile synthesis of catalysts and thin films: An introduction and summary of recent directions, Catal. Today 238 (2014) 87-94.

[16] L. dos Santos-Gómez, E.R. Losilla, F. Martín, J.R. Ramos-Barrado, D. Marrero-López, Novel microstructural strategies to enhance the electrochemical performance of $La_{0.8}Sr_{0.2}MnO_{3-\delta}$ cathodes, ACS Appl. Mater. Inter. 7 (2015) 7197-7205.

[17] J. Sar, L. Dessemond, E. Djurado, Electrochemical properties of graded and homogeneous $Ce_{0.9}Gd_{0.1}O_{2-\delta}$–$La_{0.6}Sr_{0.4}Co_{0.2}Fe_{0.8}O_{3-\delta}$ composite electrodes for intermediate-temperature solid oxide fuel cells, Int. J. Hydrog. Energy 41 (2016) 17037-17043.

[18] L. dos Santos-Gómez, J.M. Porras-Vázquez, E.R. Losilla, D. Marrero-López, Improving the efficiency of layered perovskite cathodes by microstructural optimization, J. Mater. Chem. A 5 (2017) 7896-7904.

[19] D. Marrero-López, R. Romero, F. Martín, J.R. Ramos-Barrado, Effect of the deposition temperature on the electrochemical properties of $La_{0.6}Sr_{0.4}Co_{0.8}Fe_{0.2}O_{3-\delta}$ cathode prepared by conventional spray-pyrolysis, J. Power Sources 255 (2014) 308-317.

[20] M. Guli, J. Yao, J. Zhao, W. Rao, L. Xiao, H. Tian, Preparation and characterization of TiO_2 anode film with spinodal phase separation structure in dye-sensitized solar cells, Opt. Mater. 35 (2013) 2175-2182.

[21] L. dos Santos-Gómez, J.M. Porras-Vázquez, F. Martín, J.R. Ramos-Barrado, E.R. Losilla, D. Marrero-López, Stability and performance of $La_{0.6}Sr_{0.4}Co_{0.2}Fe_{0.8}O_{3-\delta}$ nanostructured cathodes with $Ce_{0.8}Gd_{0.2}O_{1.9}$ surface coating, J. Power Sources 347 (2017) 178-185.

[22] M. Shah, S.A. Barnett, Solid oxide fuel cell cathodes by infiltration of $La_{0.6}Sr_{0.4}Co_{0.2}Fe_{0.8}O_{3-\delta}$ into Gd-Doped Ceria, Solid State Ionics 179 (2008) 2059-2064.

[23] Y. Li, W. Zhang, Y. Zheng, J. Chen, B. Yu, Y. Chen, M. Liu, Controlling cation segregation in perovskite-based electrodes for high electro-catalytic activity and durability, Chem. Soc. Rev. 46 (2017) 6345-6378.

Graphical Abstract.